Band offset and magnetic property engineering for epitaxial interfaces: A monolayer of M_2O_3 (M=Al,Ga,Sc,Ti,Ni) at the α-Fe_2O_3/α-Cr_2O_3 (0001) interface

John E. Jaffe,[1] Rafał A. Bachorz,[1,2] and Maciej Gutowski[1,3]
[1]*Chemical Sciences Division, Fundamental Sciences Directorate, Pacific Northwest National Laboratory, Richland, Washington 99352, USA*
[2]*Lehrstuhl für Theoretische Chemie, Institut für Physikalische Chemie, Universität Karlsruhe (TH), D-76128, Germany*
[3]*Chemistry School of Engineering and Physical Sciences, Heriot-Watt University, Edinburgh EH14 4AS, United Kingdom*
(Received 25 October 2006; revised manuscript received 2 March 2007; published 15 May 2007)

We have used density-functional theory with the gradient corrected exchange-correlation functional PW91 to study the effect of an interfactant layer, where Fe and Cr are replaced by a different metal, on electronic and magnetic properties of an epitaxial interface between α-Fe_2O_3 and α-Cr_2O_3 in the hexagonal (0001) basal plane. We studied a monolayer of M_2O_3 (M=Al,Ga,Sc,Ti,Ni) sandwiched with five layers of chromia and five layers of hematite through epitaxial interfaces of two types, termed "oxygen divided" or "split metal." We found that both the electronic and magnetic properties of the superlattice are modified by the interfactant monolayer. For the split-metal interface, which is favored through the growth pattern of chromia and hematite, the valence-band offset can be changed from 0.62 eV (no interfactant) up to 0.90 eV with the Sc_2O_3 interfactant, and down to −0.51 eV (i.e., the α-Fe_2O_3/α-Cr_2O_3 heterojunction changes from type II to type I) with the Ti_2O_3 interfactant, due to a massive interfacial charge transfer. The band gap of the system as a whole remains open for the interfactant monolayers based on Al, Ga, and Sc, but it closes for Ti. For Ni, the split-metal interface has a negative band offset and a small band gap. Thus, nanoscale engineering through layer-by-layer growth will strongly affect the macroscopic properties of this system.

DOI: 10.1103/PhysRevB.75.205323 PACS number(s): 73.61.Le, 73.21.Cd, 75.70.Cn, 85.75.−d

Band discontinuities are a vital aspect of electronic,[1] electro-optic,[2] and photocatalytic[3] systems made from dissimilar semiconductors. These offsets between band-gap edges at heterointerfaces depend both on the electronic structure of the two bulk compounds meeting at the interface and on the structure of the interface itself. While the interfacial structure may depend to some extent on the growth and processing history of the junction, in many cases, the band offsets can only be controlled through the choice of bulk semiconductors employed, due to symmetry constraints in epitaxial growth. However, it would be desirable to control bulk properties of the materials and interfacial offsets independently of one another. We propose to control the band offset by adding an *interfactant* layer at the interface between the main constituents of the device, analogous to a surfactant layer at a free surface. This interfactant layer should be as thin as possible, so that only the band offset is modified, and not the other device properties, assuming they are already optimal. The interfactant's atomic geometry will usually need to be consistent with the epitaxial growth of the entire structure, but the interfactant need not itself be equivalent to a particular layer cut from a stable bulk phase. Rather, it needs only to be stable (at least kinetically) in the interface structure actually desired.

Previously, band-offset control by one or more interfactant layers between traditional tetrahedrally coordinated semiconductors was considered[4] in the context of AlAs-GaAs heterostructures with elemental Ge or Si as the interfactant. Later, crystalline oxides on silicon[5] were proposed as an interfacial phase controlling junction electrostatics by means of an electrostatic dipole layer. However, our work is apparently the first to treat band-offset control by epitaxial interface chemical modification in a system containing only transition-metal oxides.

In a recent work,[6] we presented a computational study of an interface in the hexagonal (0001) plane between two antiferromagnetic semiconducting oxides, α-Cr_2O_3 (eskolaite) and α-Fe_2O_3 (hematite) whose band offset can be controlled[3] by the order in which the materials are grown. However, the maximum change in the band offset that could be obtained with only these two oxides present was about 0.4 eV experimentally.[3] In the present work, we demonstrate that the band offset can be further controlled by the presence of a monolayer of M_2O_3 M=Al, Ga, Sc, Ti, or Ni at each hematite-chromia interface. Each M_2O_3 monolayer brings a different redistribution of electron density at the interface. In consequence, the band offset can be increased or decreased, including reversal of the sign of the offset (type I to type II heterojunction transformation), and metallic interfaces may also occur when M=Ti or Ni. Significant changes to the antiferromagnetic ordering of the superlattice may also occur with the addition of interfactants, including strong ferrimagnetism.

First-principles density-functional calculations were performed with the VASP (Ref. 7) code, with the same computational conditions as in our previous[6] work. Band offsets were obtained by the same procedure[6] as before, which we describe again here in somewhat more detail. The valence-band offset for two materials connected by a prescribed interface is defined as the difference between the energies at the valence-band maxima for the two compounds, determined far from the interface. The conduction-band offset is determined similarly from the conduction-band minima, or obtained from the valence offset by adding the difference between the bulk band gaps of the two materials. For a superlattice model, it is not obvious how to directly identify the valence-band maximum (VBM) for separate regions in the

supercell occupied by the two materials, since this maximum, like other band-structure features, is not a localized quantity in real space. Instead, the usual procedure is to determine the energy of the VBM of each compound relative to a reference level that can be identified with a specific atom or localized region in a given unit cell. These reference levels are extracted from the interior or "bulklike" regions belonging to each of the two compounds in the superlattice; the VBM for each region is then assumed to "float" above the reference levels by the same amount as in the true pure bulk form of each material.

In all-electron calculations, a core-state level of an atom in an appropriate part of the system can be employed as the reference level. In pseudopotential calculations, it is more common to use a coarse-grained average of the electrostatic potential over one or more atomic layers in the bulk or bulklike region of the superlattice. We have found it convenient to instead use the average core potentials[7] supplied by the code. These potentials contain some intra-atomic effects, but their environmental dependence is mainly the additive external electrostatic potential experienced by the atom in question, and this in turn is expected to be the main determinant of the band offset. In this approach, the valence-band offset is given by

$$\Delta E^V_{C-F} = E^V_{C,bulk} - E^{core}_{C,bulk} - (E^V_{F,bulk} - E^{core}_{F,bulk}) + E^{core}_{C,superlattice} - E^{core}_{F,superlattice}, \quad (1)$$

where $E^V_{C,bulk}$ is the calculated bulk valence-band maximum for chromia, $E^{core}_{C,bulk}$ is the average core potential in bulk chromia, $E^{core}_{C,superlattice}$ is the same core potential calculated for an interior layer in the chromia region of the superlattice, and the terms with the subscript F are defined analogously for hematite. We can rearrange Eq. (1) as

$$\Delta E^V_{C-F} = [E^V_{C,bulk} - E^V_{F,bulk}] + [(E^{core}_{C,superlattice} - E^{core}_{C,bulk}) - (E^{core}_{F,superlattice} - E^{core}_{F,bulk})]. \quad (2)$$

The first expression in square brackets in Eq. (2) depends only on the choice of materials being interfaced and has the value 1.05 eV in our present calculation. The second expression in square brackets containing shifts in the core potentials is determined by the interfacial dipole layer and contains all of the dependence of Eq. (2) on the structure and composition of the interface, including any interfactant atoms placed there. We emphasize that neither bracketed expression in Eq. (2) is physically observable by itself, since both depend strongly on the details of the calculation. In our previous study,[6] we described a test calculation on a zinc-blende AlN/GaN (001) superlattice which gave a band offset in close agreement with a calculation by other workers[8] employing a coarse-grained electrostatic potential as a reference.

The model unit cell in the present study was similar to the one used in our earlier work[6]: where previously we had 6 f.u. each of Fe_2O_3 and Cr_2O_3 in the cell, we now have 5 f.u. of each of these two oxides, and 2 f.u. of the interfactant M_2O_3, where M=Al, Ga, Sc, Ti, or Ni, see Fig. 1. Each quintuple layer of Fe_2O_3 or Cr_2O_3 is thus bounded at top and bottom

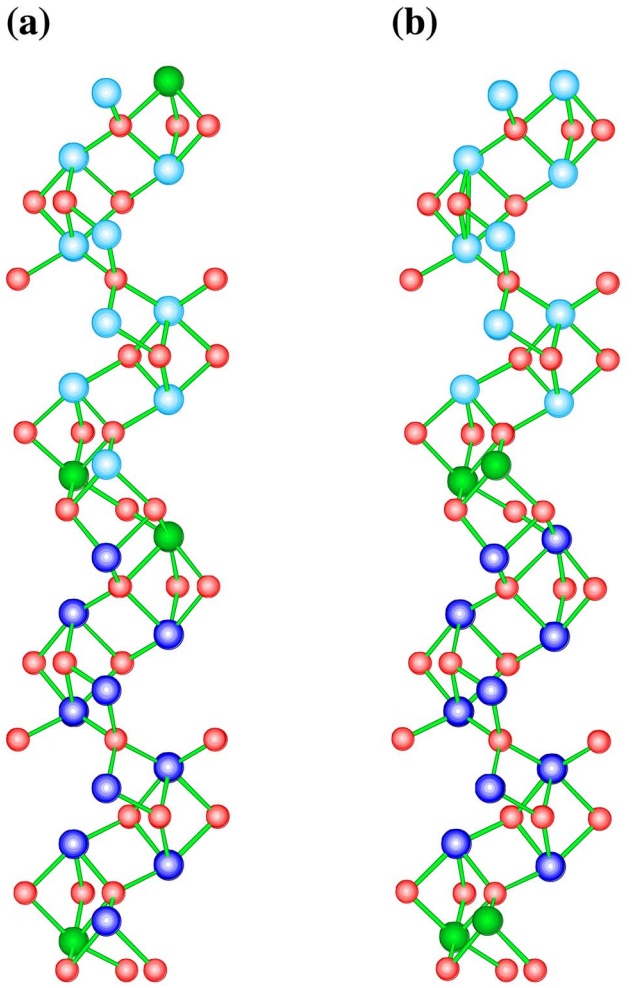

FIG. 1. (Color online) Interfacial geometry for an interfactant M_2O_3 at (a) an oxygen-divided interface between Fe_2O_3 and Cr_2O_3, producing a split-metal interface between the host oxides and the interfactant, and (b) at a split-metal interface between Fe_2O_3 and Cr_2O_3, producing an oxygen-divided interface between the host oxides and the interfactant. Each pair of M atoms (solid spheres) replaces one Fe (dark shaded spheres in the lower half of the figure) and one Cr (light shaded spheres) of the unmodified superlattice. The smaller spheres represent oxygen atoms.

[with respect to the hexagonal (0001) axis] by a layer of M_2O_3. In the corundum structure, oxygen atoms lie in triangular nets in planes normal to (0001), while the metal atoms lie in puckered double layers or "bilayers" between the oxygen planes. Previously, we identified two possible interfaces between α-Fe_2O_3 and α-Cr_2O_3 along (0001): an "oxygen-divided" one in which an oxygen plane at the interface separates an iron bilayer from a chromium bilayer, and a "split-metal" interface in which there is a metal bilayer at the interface, containing an iron single layer on the hematite side and a chromium single layer on the α-Cr_2O_3 side. We now form interfactant layers in each kind of interface by replacing 1 f.u. of $FeCrO_3$ by the interfactant M_2O_3. When we do this at the oxygen-divided interface between α-Fe_2O_3 and α-Cr_2O_3, the result is a split-metal interface between α-Cr_2O_3 and M_2O_3 followed by another split-metal interface

TABLE I. Cr_2O_3-Fe_2O_3 valence-band offsets (BOs) in eV, magnetization of the unit cell (mag) in units of electron spin, and interfactant metal (M) Pauling electronegativities (ENs). SM=split-metal native-interfactant interface; OD=oxygen-divided native to interfactant interface. The first band offset is the first-principles value; the second (in parentheses) is an approximation derived from a simple electrostatic model using an atomic charge population analysis described in the text.

		SM		OD	
M	EN[a]	BO	mag	BO	mag
None		0.62(0.43)	0.00	0.40(0.34)	0.00
Al	1.5	0.72(0.80)	0.00	0.54(0.34)	−10.00
Ga	1.6	0.78(0.30)	0.00	0.59(0.65)	−10.00
Sc	1.3	0.90(0.74)	0.00	0.59(0.38)	−10.00
Ti	1.5	−0.51(−1.57)	0.01	−0.47(−1.28)	−6.07
Ni	1.9	−0.14(−0.96)	0.00	0.03(−0.25)	−3.07

[a]Reference 9. The electronegativities of Cr and Fe are 1.6 and 1.8, respectively.

between M_2O_3 and α-Fe_2O_3. Conversely, when we do the same replacement at the split-metal interface in the host superlattice, we obtain oxygen-divided interfaces between the interfactant and the host oxides. We show a ball-stick diagram of superlattices with (a) split-metal and (b) oxygen-divided interfaces to the interfactant in Fig. 1. Relaxation of all structures to their energy minima produced only small shifts of 0.03 Å or less from the atomic positions in the unsubstituted superlattice.

We give the calculated valence-band offsets for the fully relaxed interfactant structures in Table I. A positive band offset means that the VBM for chromia is above that of hematite, consistent with a type II heterojunction. Interfactant metal-atom electronegativities[9] and calculated lattice magnetic properties are also included and will be discussed below. For the Ti_2O_3 split-metal interfactant case, we performed an additional calculation with a unit cell 1.5 times longer along the c axis than the other cases and found a band offset within approximately 0.1 eV of that given in Table I. Recomputing the bulk VBM and core potentials with the relaxed in-plane lattice constant taken from this supercell calculation only caused changes on the order of 0.05 eV in the offset.

For the trivalent substituents M=Al,Ga,Sc, the effect of the interfactant is to increase the band offset for both starting interfaces by similar but not identical amounts. For the nominally tetravalent Ti and divalent Ni, we see far more dramatic changes in the band offsets, including strongly negative VB offset (type I heterojunction) for Ti. We attribute this effect to a large electron transfer from Ti (now in a trivalent environment) to the Fe conduction-band states near the interface. The resulting surface dipole layer raises the energy of the Fe 3d-dominated states below the superlattice valence-band maximum relative to the Cr 3d-like states at the valence-band maximum to the extent that it reverses the sign of the valence-band offset. The addition of charge to the conduction-band minimum also produces a metallic (conducting) layer near the interface. The situation for the Ni_2O_3 interfactant appears to be opposite from Ti_2O_3 in that now there is an electron transfer *to* the interfactant layer. In this case, however, the negative charge is transferred from the Cr-dominated valence-band maximum, lowering its energy until the highest occupied Cr and Fe states are nearly degenerate, that is, the original positive (Cr above Fe) valence-band offset is again reduced or reversed. For Ni, a metallic or semimetallic (but now p-type) state again occurs.

Large changes in the magnetic structure of the superlattice can occur when selected Cr and Fe atoms are replaced by the interfactant metal, as shown in Table I. Bulk Fe_2O_3 and Cr_2O_3 are both antiferromagnetic, but the Cr spins in Cr_2O_3 alternate both within the bilayers and along the c axis, while in hematite they alternate only along the c axis, with individual Fe bilayers ordered ferromagnetically (here, we neglect the low-temperature canted weak ferrimagnetism in hematite). In the unsubstituted Fe_2O_3/Cr_2O_3 superlattice, there are six Fe bilayers in each unit cell, so the net spin moment is zero. The superlattice shown in Fig. 1(a) with the split-metal host/interfactant interface contains four Fe bilayers, and the two Fe atoms in the interfacial (mixed) bilayers will also have an opposite spin to each other; thus, the net moment is again nearly zero. However, in the superlattice shown in Fig. 1(b), there are instead five complete Fe bilayers. Since these bilayers alternate spin up and spin down, and there are odd numbers of them in the cell, the cell has a large spin moment, as shown in Table I. This situation is modified for M=Ti and Ni. For Ti, there is one electron per Ti transferred to the minority-spin Fe bands; thus, the magnitude of the net spin is reduced from 10 to 6. In the case of Ni, one must also consider the contribution of the Ni 3d bands. We find that the Ni atoms adopt low-spin moments intermediate between what one would expect for the Ni^{2+} and Ni^{1+} atomic charge states. In the structure of Fig. 1(a), the Ni spins follow the antiferromagnetic spin order of the nearest host transition-metal atoms, so that their net contribution to the total spin moment of the cell is zero. On the other hand, in the structure of Fig. 1(b), the Ni atoms in the interfactant bilayers follow the spin order of hematite, that is, ferromagnetic within bilayers but alternating along the c axis between bilayers. These polarized interfactant layers have spins in the opposite direction to the majority of Fe spins, but they do not reverse or cancel the net polarization, rather they simply reduce it since the spin state of Fe is formally 5 but for Ni it is

between 1 and 2 on the average. There is also some enhanced occupation of Fe minority-spin states which further reduces the net moment, as shown in Table I, to around 3 electron spins.

To account in more detail for the origins of the predicted band offsets, we performed a charge population analysis by the spatial partitioning method of Bader and Nguyendang,[10] then treated each atom as a point charge including its pseudopotential core-nuclear charge. Assigning these charges to planes parallel to the interface, we used Gauss's law to obtain an approximation to the smoothed electrostatic potential difference between the interior of the Fe_2O_3 region and the interior of the Cr_2O_3 region in the superlattice. This electrostatic contribution is added to the first expression in square brackets in Eq. (2), i.e., the 1.05 eV difference between the valence-band maxima of bulk Cr_2O_3 and Fe_2O_3, resulting in the approximate band-offset numbers given in parentheses in Table I. The semiquantitative agreement with offsets found directly from core potentials confirms that electron transfer from the Cr_2O_3 to the Fe_2O_3 side of the interface is the main factor in the interfactant effects on the band offset. In the unsubstituted superlattice, there was a net charge transfer on the order of 0.02 electrons across the interface, mostly from the Cr bilayer nearest the interface to its Fe counterpart on the other side, lowering the electrostatic potential on the Fe side by several tenths of a volt relative to the Cr side (i.e., raising the electron energy levels by an equal amount in eV.) Since the valence-band edge on the Cr side would otherwise be 1.05 eV higher than on the Fe side, the offset is reduced by several times 0.1 eV. The downshift is slightly greater for the O-divided interface, in part because the layers involved in the transfer are further apart, creating a larger surface dipole. However, this small charge transfer is associated with polarization of bonding charge toward the Fe side and not with a change in orbital occupation.

When the Al_2O_3, Ga_2O_3, and Sc_2O_3 interfactant layers are substituted into the superlattice, the electrostatic downshift of the valence-band offset is reduced, because identical interfactant metal atoms are replacing Fe on one side of the interface and Cr on the other side. The effect may be greatest for Sc because it has the largest atomic radius of the trivalent interfactant metals considered, so that the layer of Sc_2O_3 isolates the host oxides from each other slightly more; the net transfer is only about 0.01 electrons per cell in this case.

When the interfactant metal is Ti or Ni, the effect is much larger because there are now formally two excess electrons per unit supercell from Ti that must be accommodated in Fe-derived conduction-band interfacial states, or two electrons that must be transferred from Cr-derived interfacial states toward the Ni layers. (The charge transfers found by the population analysis are roughly 0.2 electrons for Ti and 0.1 electrons for Ni, much less than the formal valence difference since the charge is actually delocalized over several atomic layers in the interfacial zone, and atomic polarization is not taken into account.) In either case, the net effect is a transfer of electrons from the Cr layers toward the Fe layers, but now of such magnitude that the band offset is depressed until it changes sign.

In summary, we have shown that large, macroscopically measurable modifications to the electronic and magnetic properties of α-Fe_2O_3/α-Cr_2O_3 heterojunctions are possible through the placement of an interfactant layer of a different oxide. With present-day layer-by-layer molecular-beam epitaxy techniques,[11] creation of such structures should be quite feasible. This is the first time such an interfacial modification has been proposed for oxides, and the magnetic effects have no counterpart in traditional semiconductors[4,5,8] where interface modifications have been considered before. The split-metal host to interfactant structure [Fig. 1(a)] is likely to be more easily realized experimentally, due to the electrostatic stabilization of the half-metal-bilayer termination of the corundum structure (0001) surface. However, by careful control of oxygen partial pressure and other growth conditions, it may prove possible to form the other structure [Fig. 1(b)] as well. The resulting large uncompensated spin moments may then prove useful in spintronic[12] device development.

This work was supported by the U.S. Department of Energy, Office of Basic Energy Sciences, Chemical Sciences program. PNNL is operated by Battelle for the U.S. DOE under Contract No. DE-AC06-76RLO 1830.

[1] J. Robertson, Rep. Prog. Phys. **69**, 327 (2006).
[2] F. Ishikawa, M. Horicke, U. Jahn, A. Trampert, and K. H. Ploog, Appl. Phys. Lett. **88**, 191115 (2006).
[3] S. A. Chambers, Y. Liang, and Y. Gao, Phys. Rev. B **61**, 13223 (2000).
[4] G. Bratina, L. Sorba, A. Antonini, G. Biasiol, and A. Franciosi, Phys. Rev. B **45**, 4528 (1992); L. Sorba, G. Bratina, A. Antonini, A. Franciosi, L. Tapfer, A. Migliori, and P. Merli, *ibid.* **46**, 6834 (1992); G. Biasiol, L. Sorba, G. Bratina, R. Nicolini, A. Franciosi, M. Peressi, S. Baroni, R. Resta, and A. Baldereschi, Phys. Rev. Lett. **69**, 1283 (1992).
[5] R. A. McKee, F. J. Walker, M. Buongiorno Nardelli, W. A. Shelton, and G. M. Stocks, Science **300**, 1726 (2003).
[6] J. E. Jaffe, M. Dupuis, and M. Gutowski, Phys. Rev. B **69**, 205106 (2004).
[7] G. Kresse and J. Hafner, Phys. Rev. B **47**, 558 (1993); **48**, 13115 (1993); **49**, 14251 (1994); J. Phys.: Condens. Matter **6**, 8245 (1994); G. Kresse and J. Furthmüller, Comput. Mater. Sci. **6**, 15 (1996); Phys. Rev. B **54**, 11169 (1996) and references therein.
[8] S.-H. Wei and A. Zunger, Appl. Phys. Lett. **72**, 2011 (1998) and references therein.
[9] L. Pauling, *General Chemistry* (Dover, New York, 1988), p. 182.
[10] R. F. W. Bader and T. T. Nguyendang, Adv. Quantum Chem. **14**, 63 (1981).
[11] S. A. Chambers, J. R. Williams, M. A. Henderson, A. G. Joly, M. Varela, and S. J. Pennycook, Surf. Sci. **587**, L197 (2005).
[12] S. A. Wolf, D. D. Awschalom, R. A. Buhrman, J. M. Daughton, S. von Molnar, M. L. Roukes, A. Y. Chtchelkanova, and D. M. Treger, Science **294**, 1488 (2001).